Volume 47 | Number 29 | 7 August 2018 | Pages 9557–9914

Dalton Transactions

An international journal of inorganic chemistry

rsc.li/dalton

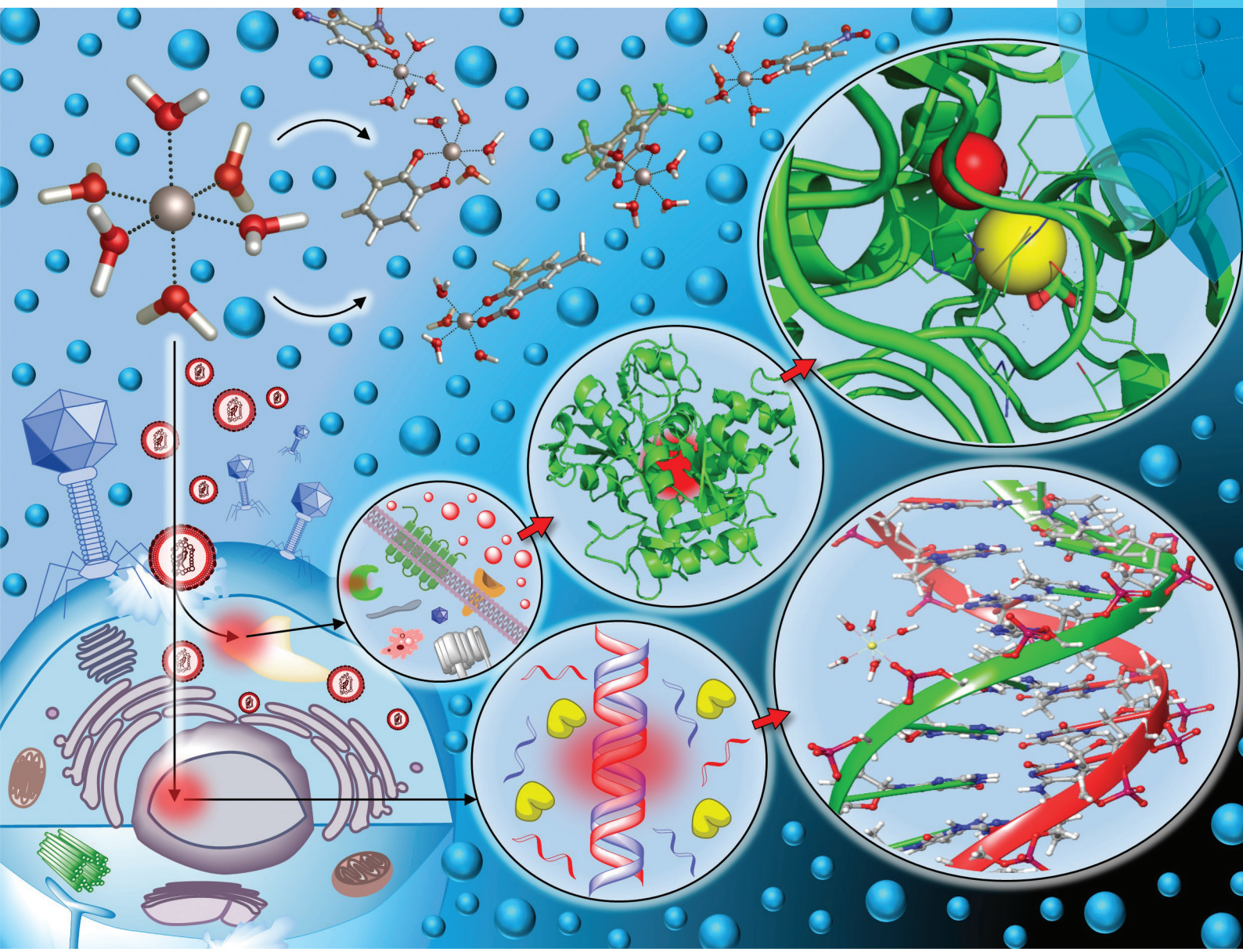

ISSN 1477-9226

ROYAL SOCIETY OF CHEMISTRY

PAPER

Xabier Lopez *et al.*

Tuning the affinity of catechols and salicylic acids towards Al(III): characterization of Al–chelator interactions

Dalton Transactions

PAPER

View Article Online
View Journal | View Issue

Cite this: *Dalton Trans.*, 2018, **47**, 9592

Tuning the affinity of catechols and salicylic acids towards Al(III): characterization of Al–chelator interactions†

Gabriele Dalla Torre, [a,b] Jon I. Mujika, [a] Elena Formoso, [a] Eduard Matito, [a,c] Maria J. Ramos [b] and Xabier Lopez*[a]

Due to aluminum's controversial role in neurotoxicity, the goal of chelation therapy, the removal of the toxic metal ion or attenuation of its toxicity by transforming it into less toxic compounds, has attracted considerable interest in the past years. In the present paper we present, validate and apply a state-of-the-art theoretical protocol suitable for the characterization of the interactions between a chelating agent and Al(III). In particular, we employ a cluster-continuum approach based on Density Functional Theory calculations to evaluate the binding affinity of aluminum for a set of two important families of aromatic chelators: salicylic acids and catechols. Our protocol shows very good qualitative agreement between the computed binding affinities and available experimental stability constants ($\log\beta$) values for 1 : 1, 1 : 2 and 1 : 3 complexes. Then, we have investigated the nature of the Al–O bond in an enlarged dataset of 27 complexes of 1 : 1 stoichiometry, by means of the QTAIM and Energy Decomposition Analysis (EDA). Quite interestingly, we have found that although the Al–O interaction is mainly electrostatic, there is a small but significant degree of covalency that explains the modulation of binding affinities in both families of compounds by the addition of electron donating (CH_3, OCH_3) or withdrawing (NO_2, CF_3) substituents. The role of aromaticity and the mechanisms of action of the different functional groups were also evaluated. Finally, we have analyzed the competition between Al(III) and proton toward the binding of these chelators, giving a rationalization of the different trends found experimentally between $\log\beta$ and the amount of free aluminum in solution in the presence of a given ligand (p[Al]). In summary, we propose a validated and comprehensive computational protocol that can provide a valuable help toward the design and tuning of new efficient aluminum chelators.

Received 6th April 2018,
Accepted 16th May 2018

DOI: 10.1039/c8dt01341a

rsc.li/dalton

Introduction

Aluminum is the third most abundant element in the Earth's crust, following oxygen and silicon. However, complex but effective geochemistry has prevented its solubilization,[1,2] allowing biological systems to evolve in the absence of this abundant metal. Nonetheless, in the past century, human intervention has made aluminum bioavailable in a myriad different ways, and as a consequence, important trace amounts of this element are found in the human body. The introduction of a nonessential element into biological cycles has raised justified concerns about its biological effects and potential toxicity,[3–5] and the scientific literature on the adverse health effects of aluminum is extensive.[6] Although the exact mechanisms of aluminum toxicity are not well understood at the atomic level, there is increasing evidence that aluminum promotes oxidative stress,[7–9] inhibits the normal function of several enzymes (such as hexokinase,[10] glutamate dehydrogenase,[11–13] *etc.*), interferes with several key cell metabolism cycles,[14–16] and alters the structure and chemistry of important metabolites[12] and cofactors.[17] Aluminum is also considered a neurotoxic element.[18] Early studies supported this hypothesis, linking aluminum and the formation of neurofibrillary tangles (NFT).[19] In fact, both experimental and theoretical studies have underlined the ability of aluminum to bind to phosphorylated peptides[20,21] and to promote the hyperphosphorylation of normal neurofilaments.[22] In addition, the ability of aluminum to contribute to Aβ-amyloid aggregation has been recently demonstrated,[23,24] and growing

[a]*Kimika Fakultatea, Euskal Herriko Unibertsitatea UPV/EHU, and Donostia International Physics Center (DIPC), P.K. 1072, 20080 Donostia, Euskadi, Spain. E-mail: xabier.lopez@ehu.es*
[b]*UCIBIO/REQUIMTE, Departamento de Química e Bioquímica, Faculdade de Ciências, Universidade do Porto, Rua do Campo Alegre, s/n, Porto, Portugal*
[c]*IKERBASQUE, Basque Foundation for Science, 48013 Bilbao, Euskadi, Spain*
†Electronic supplementary information (ESI) available. See DOI: 10.1039/C8DT01341A

evidence links aluminum to be a decisive contributing factor in Alzheimer's disease.[25–27]

In this controversial context, the quest for chelating agents that could be an effective treatment for aluminum-related disorders has attracted considerable interest.[28–32] In particular, catechols and salicylic acids have emerged as very promising building blocks for the design of effective aluminum chelators, because they constitute two of the strongest bidentate aluminum binding species.[33] The reason for that relies on the fact that Al(III) is a hard Lewis acid (and the hardest trivalent metal), and therefore it prefers to coordinate to hard Lewis bases such as phenoxide and carboxylate.[33] Moreover, the interaction of aluminum with such functional groups is supposed to be mainly electrostatic in nature.[30] Due to this inherent affinity, it is not surprising that the biochemistry of important neurotransmitters like catecholamines is highly affected by the presence of aluminum.[34–36] It has been shown that aluminum affects the signaling process mediated by these neurotransmitters,[37] it alters their content in animal models,[34] and it interferes with enzymatic activities that involve these neurotransmitters.[38,39] Because of their strong binding affinity, both catechols and salicylic acids have been extensively studied[28,30,40,41] in the framework of aluminum chelation therapy with the aim of finding improved and aluminum-specific chelators by tuning their chemical environment with different substituents. The efficiency of low molecular mass aluminum–chelator complexes has been studied by means of several experimental techniques, such as potentiometric titrations, UV/Vis spectroscopy, ^{1}H NMR and ESI-MS.[40–44] Nevertheless, the effects mediated by the inclusion of different substituents in the molecule and how they may modulate the binding affinity toward aluminum are still not well understood.[41,43] In this sense, the understanding of the effect of electron withdrawing groups (EWGs) and electron donating groups (EDGs), the role played by aromaticity in these chelators, the rationalization of complex stability, and the specific nature of the Al–O bonds is of paramount importance to guide the quest for improved aluminum chelating agents. However, often this relevant information cannot be deduced directly from experimental procedures alone.

The use of state-of-the-art theoretical methods can provide valuable insights into the properties of these systems, as demonstrated elsewhere.[45–47] In the present work, we present a comprehensive computational protocol to investigate the behavior of different chelating agents interacting with Al(III). Validation with respect to available experimental data is also performed. Then, the validated protocol is applied to the characterization of the substituent effects and the bonding nature of various aluminum–chelator complexes, as well as their aromatic-related properties, in order to provide a thorough rationalization of the behavior of these chelators. We have considered two main families of chelating agents, salicylic acids and catechols, bearing electron donating groups (EDGs, methyl and methoxy) and electron withdrawing groups (EWGs, nitro and trifluoromethyl) placed at different positions along the aromatic ring and in different quantities (see Fig. 1 and Table 2). These substituents were chosen since they exert opposite effects through different mechanisms of action (resonance and/or induction). Our results demonstrate that although the Al–O bond is mainly of an ionic nature, as it corresponds to a hard metal ion, the trend in the stability for these complexes is mainly determined by covalent dative interactions. We also analyze how Al(III)/proton competition modulates the properties of these chelators.

Methods

The computational protocol that we developed for the investigation of different Al(III)–chelator complexes is outlined in Fig. 2 and presented in the following sections. For the sake of simplicity, we provide only a schematic overview of the whole protocol; therefore, for the full theory and technical details of each methodology we redirect the reader to the specific computational details section in the ESI.†

Definition of binding affinities: cluster-continuum approach

In order to investigate the thermodynamics of all Al(III)–chelator complexes in aqueous solution, we utilized the so-called cluster-continuum approach,[48–50] with the first-coordination shell of aluminum surrounded by explicit water molecules in an octahedral fashion and the effects of the remaining solvent considered with a continuum dielectric model (see Fig. 4). Optimization and single point calculations were performed at the B3LYP-D3(BJ)/6-311++G(3df,2p)//B3LYP-D3(BJ)/6-31++G(d,p) level using the integral equation formalism variant (IEFPCM) solvation model.[51] Such a choice was made since it has been shown that the introduction of dispersion corrections on both geometry and single point energy calculations improve the overall results.[52] In general, the addition of methods that properly take into account dispersion energies in DFT has been proven to improve the precision of computed non-covalent interactions.[53,54] For results with different density functionals and the MP2 method and their evaluation *versus* experimental stability constants see ESI Tables S1–S5 and Fig. S1–S2.†

We characterized bidentate Al–Lig complexes with 1 : 1, 1 : 2 and the 1 : 3 stoichiometry following the ligand substitution reaction shown in (1):

$$[Al(H_2O)_6]_{(aq,1\,M)}{}^{3+} + L_{r(aq,1\,M)}{}^{q-} \rightarrow [Al(H_2O)_{6-m}L_r]_{(aq,1\,M)}{}^{3-q} + mH_2O_{(aq,1\,M)} \quad (1)$$

where q is the net charge of the ligand L, r is the number of ligands and m depends on the stoichiometry of the complex, such as m = 2, m = 4 and m = 6 for 1 : 1, 1 : 2 and 1 : 3 complexes, respectively. Notice that we consider the ligand in its unprotonated form, which is the state considered when evaluating experimental log(β) (the validation of binding affinities section).

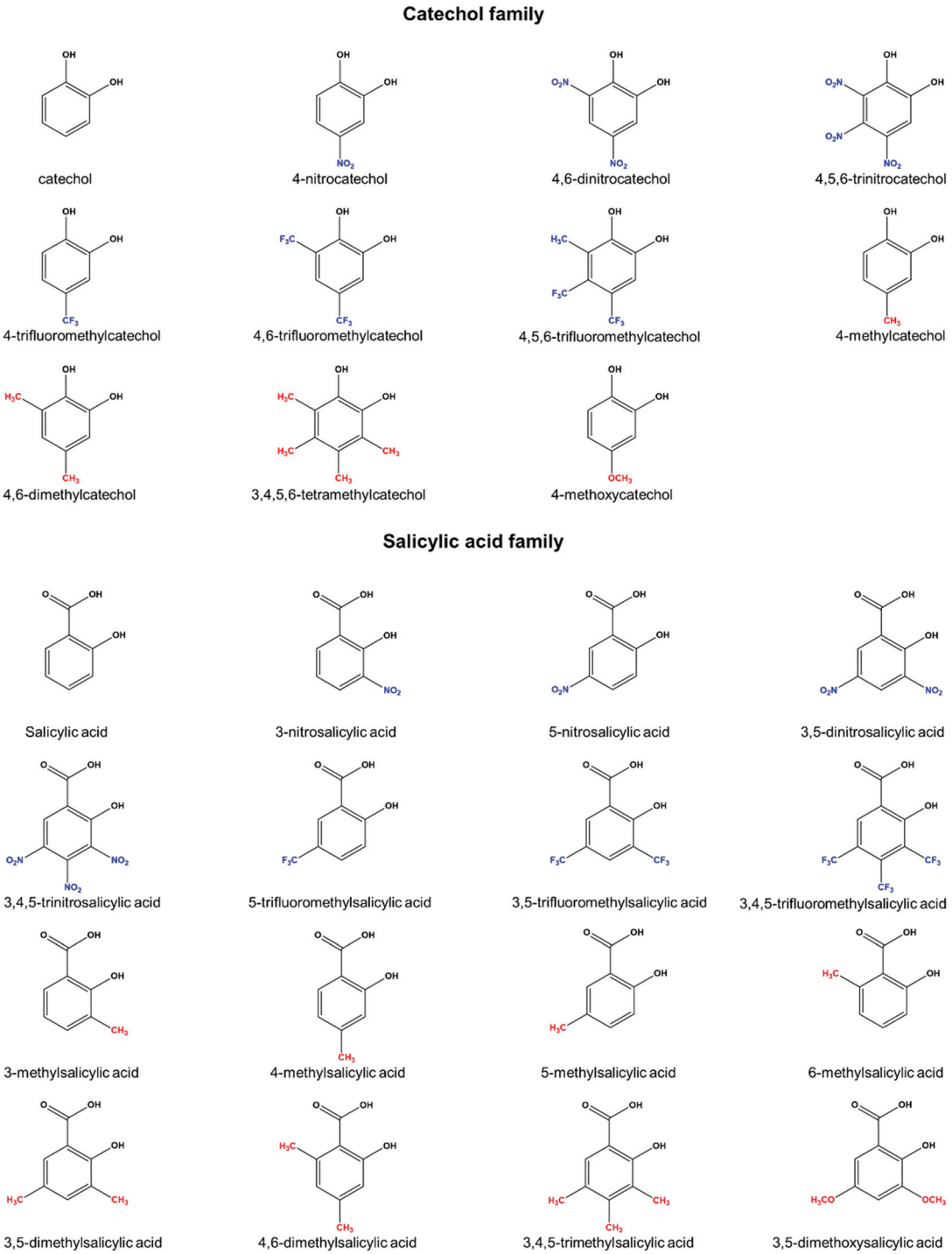

Functional group	*Inductive*	*Resonance*	*Overall*
Methyl (-CH_3)	ED	-	EDG
Methoxy (-OCH_3)	EW	ED	EDG
Nitro (-NO_2)	EW	EW	EWG
Trifluoromethyl (-CF_3)	EW	-	EWG

Fig. 1 Summary of the two families of chelators with the four different substituents considered in this work: methyl and methoxy (EDGs), nitro and trifluoromethyl (EWGs). The different mechanisms of action of the substituents are also summarized.

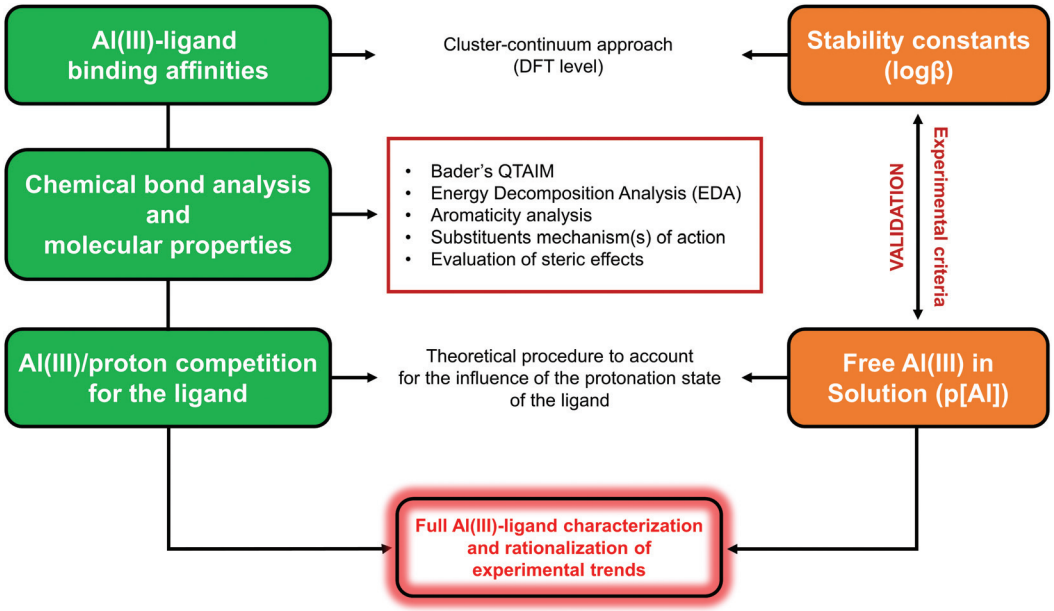

Fig. 2 Schematic representation of the theoretical protocol developed in this work.

The enthalpy in solution corresponding to the binding of the ligand to Al(III) is therefore calculated as:

$$\Delta H_{aq}^{comp} = H_{aq}[Al(H_2O)_{6-m}L_r] + mH_{aq}(H_2O) - H_{aq}[Al(H_2O)_6] - H_{aq}(L)_r + \Delta nRT\ \ln(24.46) \quad (2)$$

Since the enthalpies are determined using an ideal gas at 1 atm as the standard state, the last term in eqn (2) corresponds to the volume change due to the transformation from 1 atm to 1 M in solution, where Δn refers to the change in the number of species in the reaction.[55] In a similar way, the free energy of the complexes is determined as:

$$\Delta G_{aq}^{comp} = G_{aq}[Al(H_2O)_{6-m}L_r] + mG_{aq}(H_2O) - G_{aq}[Al(H_2O)_6] - G_{aq}(L)_r + \Delta nRT\ \ln(24.46) + mRT\ \ln(55.34) \quad (3)$$

where the last term is the entropic factor that accounts for the concentration of 55.34 M of water in liquid water.[55]

The validation of binding energies with respect to experimental stability constants (*i.e.* $\log\beta$) is thoroughly discussed in the validation of binding affinities section.

Chemical bond analysis and evaluation of molecular properties

At the second stage, to provide a quantitative and qualitative characterization of the interactions arising in these Al(III)–chelator complexes, as well as to unveil the effect of different substituents (EDGs and EWGs) toward complex stability, we have employed several state-of-the-art computational techniques summarized as follows:

• **Quantum Theory Of Atoms In Molecules (QTAIM):** Bader's theory[56] allows the classification of the nature of a given bond according to the characteristics of its Bond Critical Point (BCP), such as the electron density at the BCP $\rho(r_{BCP})$, the Laplacian of the electron density $\nabla^2\rho(r_{BCP})$ and the total energy density $H(r_{BCP})$. Delocalization Indices (D.I.$_{AB}$) provide a mean of the average number of electron pairs shared between two atoms A and B.

• **Energy Decomposition Analysis (EDA):** The EDA scheme by Morokuma[57] and Ziegler and Rauk[58] decomposes the total interaction energy (ΔE_{int}) between two molecules into three main components, that is, an electrostatic interaction term (ΔE_{elstat}), an orbital interaction term (ΔE_{oi}) and a Pauli repulsion term (ΔE_{Pauli}). Therefore, the EDA scheme allows the measurement and quantification of the electrostatic and covalent effects that may arise in a given complex.

• **Aromaticity analysis:** The analysis of the aromaticity of a molecule according to the I_{ring}[59] and MCI[60] aromatic descriptors is useful to compare the overall aromatic character of a given ligand with respect to a reference (*i.e.* benzene for an aromatic compound, cyclohexane for a non-aromatic one); moreover, it is possible to analyze the effects that the addition of substituents of different nature may have on the aromatic-based properties (like resonance) of the ligand, so as to provide a rationale for their mechanism of action.

• **Evaluation of possible steric effects:** Steric hindrances may take place between two or more functional groups placed close to one another; accordingly, it is important to evaluate the change in stability due to repulsive phenomena upon the addition of bulky functional groups.

Aluminum ion and proton competition

Finally, we developed a strategy to account for the influence of the protonation constants of a given ligand toward the stability of the complex with Al(III), and, therefore, for the competition between Al(III) and the proton for the ligand. The latter aspect

is particularly important upon addition of substituents because different functional groups lead to different effects against ligand's pK_a, modulating the overall basicity/acidity of the chelator.[40,41,61] The whole strategy is presented and discussed in the proton and aluminum ion competition section, and its evaluation and validation with respect to the experimental p[Al] criteria is also provided.

Results and discussion

Validation of binding affinities

Experimentally, chelation affinity is usually measured using two different criteria: p[M] and $\log\beta$ (cumulative stability constant).[62] p[M] is defined as the negative logarithm of the concentration of the free metal in solution, calculated for total [ligand] = 10^{-5} M and total [metal] = 10^{-6} M at pH 7.4, usually calculated from data at 25 °C and 0.1 M ionic strength.[63] This criteria is usually useful when comparing different chelators, as p[M] takes into account the effects of ligand protonation and denticity, so that it can provide a general and qualitative insight about the chelation properties of the molecule in solution.[62–64] On the other hand, stability constants ($\log\beta_{abc}$) can be expressed as $a\mathrm{M} + b\mathrm{L} + c\mathrm{H} \rightleftharpoons \mathrm{M}_a\mathrm{L}_b\mathrm{H}_c$, where M is the metal, L is the ligand (in its unprotonated form) and H stands for a given protonation state. In other words, this is a measure of the strength of the interaction between the metal and the ligand that form the complex.

In order to validate our approach, theoretical binding energies of 1 : 1, 1 : 2 and 1 : 3 complexes were evaluated with respect to the available experimental $\log\beta$ and p[Al] values taken from ref. 40. At this stage, those complexes with available experimental data were included, namely: catechol, 4-nitrocatechol, salicylic acid, 3-nitrosalicylic acid, 5-nitrosalicylic acid and 3,5-dinitrosalicylic acid. Optimized geometries are shown in Fig. 4, and the ΔG_{aq}^{comp} and ΔH_{aq}^{comp} values reported in Table 1 along with experimental data.

As we can see in Fig. 3, our theoretical protocol is able to describe the relative affinity for this set of molecules. Indeed, theoretical ΔG_{aq}^{comp} shows the same trends as the experimental $\log\beta$ for all stoichiometries, with a total correlation coefficient of 0.9692. On the other hand, if we analyze the trends observed for p[Al] (Table 1), we can see that these trends are not the same order as for $\log\beta$ and ΔG_{aq}^{comp}. Notice that p[Al] does not depend on the stoichiometry (Table 1); indeed, it is often used

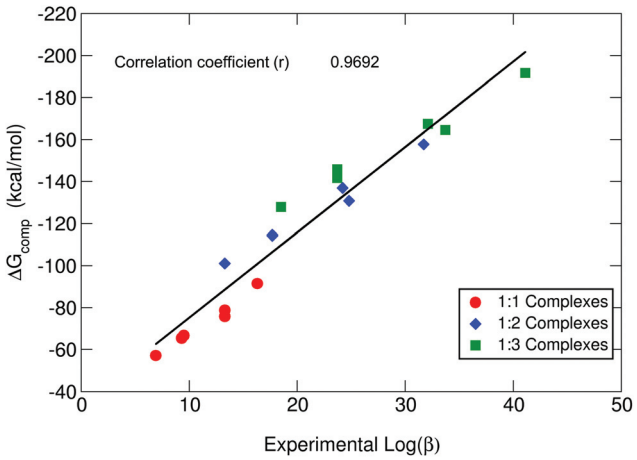

Fig. 3 B3LYP-D3(BJ) binding energies (ΔG_{aq}^{comp}) *versus* experimental stability constants ($\log\beta$).[40]

Table 1 Binding enthalpies (ΔH_{aq}^{comp}) and free energies (ΔG_{aq}^{comp}) in kcal mol^{-1} calculated for 1 : 1, 1 : 2 and 1 : 3 Al–ligand complexes with available experimental log(β) and p[Al] data, taken from ref. 40

			Theoretical		Experimental	
Stoichiometry		Ligand	ΔH_{aq}^{comp}	ΔG_{aq}^{comp}	log(β)	p[Al]
1 : 1 Complexes	Catecholates	Catecholate	−88.4	−91.4	16.3	10.1
		4-Nitrocatecholate	−71.6	−75.8	13.3	14.2
	Salicylates	Salicylate	−76.9	−78.7	13.3	8.2
		3-Nitrosalicylate	−64.2	−66.7	9.5	8.7
		5-Nitrosalicylate	−63.3	−65.4	9.3	8.4
		3,5-Dinitrosalicylate	−55.0	−57.1	6.9	9.1
1 : 2 Complexes	Catecholates	Catecholate	−151.8	−157.7	31.7	10.1
		4-Nitrocatecholate	−124.0	−130.8	24.8	14.2
	Salicylates	Salicylate	−130.8	−136.9	24.2	8.2
		3-Nitrosalicylate	−110.6	−114.6	17.7	8.7
		5-Nitrosalicylate	−109.2	−114.2	17.7	8.4
		3,5-Dinitrosalicylate	−95.4	−101.0	13.3	9.1
1 : 3 Complexes	Catecholates	Catecholate	−183.1	−191.7	41.1	10.1
		4-Nitrocatecholate	−154.8	−164.6	33.7	14.2
	Salicylates	Salicylate	−160.6	−167.5	32.1	8.2
		3-Nitrosalicylate	−139.8	−145.8	23.7	8.7
		5-Nitrosalicylate	−137.8	−141.7	23.7	8.4
		3,5-Dinitrosalicylate	−125.8	−127.9	18.5	9.1
Total correlation coefficients					0.9692	0.1235

as an indirect ligand affinity indicator.[64] However, the observed discrepancies between p[Al] and $\log\beta$ are due to the fact that, as previously mentioned, p[Al] depends not only on the stability of the complexes, but also on other factors like metal/proton competition, the number of different Al(III)–chelator species present at pH 7.4 and the denticity of the chelator.[62,64] This denotes the limits of using p[M] alone, as a unique measure of complex stability. A more detailed discussion about p[Al] is provided in the proton and aluminum ion competition section.

Optimized geometries for 1 : 1, 1 : 2 and 1 : 3 complexes can be found in Fig. 4. In all complexes the ligands interact bidentately with aluminum. Since Al(III) is always hexacoordinated, the remaining coordination sites are filled with water molecules. In 1 : 1 and 1 : 2 complexes, aluminum is always placed coplanar to the aromatic rings. In 1 : 2 complexes, the two ligands are not fully coplanar as they are slightly tilted towards one another (deviation dihedrals in the 8.0–11.0 degree range, Fig. 4). In the case of 1 : 3 complexes, whereas the catechol family still retains the coplanarity (Fig. 4) of aluminum with respect to the aromatic rings, salicylic acid complexes show slight distortions, due to π–π stacking interactions that arise between the adjacent aromatic rings.

Finally, we would like to point out that we repeated our calculations with other dispersion corrected DFT functionals, as well as at the MP2 level of theory (see ESI Tables S1–S5 and Fig. S1 and S2†), finding a good agreement between all different methods and B3LYP-D3(BJ) binding energies, which further validates our approach.

Modulation of the binding affinities by electron donating and withdrawing groups

Once our theoretical binding energies were validated with respect to available stability constants, and taking into account that the relative affinities are not affected by the different stoichiometries, we focus on 1 : 1 complexes and enlarge our dataset of possible chelators by considering the four types of substituents presented in Fig. 1: methyl and methoxy (EDGs), and nitro and trifluoromethyl (EWGs). These substituents were placed at different positions of the catecholate/salicylate rings, and in different quantities. In this way, a total of 27 complexes were considered (1 : 1 complexes of Fig. 4 and 5). Results can be found in Table 2.

Our results show that the inclusion of methyl and methoxy groups leads to larger binding energies when compared with the unsubstituted compounds of both families, whereas the inclusion of nitro and trifluoromethyl groups leads to lower affinities. The destabilizing effect of the inclusion of a nitro group is larger than the destabilizing effect of a trifluoromethyl group and, moreover, larger than the stabilizing effect of the inclusion of both methyl/methoxy groups. This can be qualitatively explained in terms of inductive and resonance effects (see Fig. 1): nitro is an EWG by both inductive and resonance effects, whereas trifluoromethyl is an EWG only by induction. Moreover, methoxy shows contrary effects that partially compensate, *i.e.* an electron withdrawing effect by induction and a donating one by resonance. Finally, methyl is electron donating only by the inductive effect. As we will see in the role of aromaticity section, resonance effect dominates over inductive effect and methoxy has an overall electron donating behavior. Our results are consistent with the hypothesis by Nurchi *et al.*[40] in that the decrease in the stability constants caused by the nitro substituent was due to a mixture of inductive/resonance effects. On the other hand, in a more recent paper, Nurchi *et al.*[41] also pointed to the increase in the stability of complexes formed by methoxysalicylic acids and aluminum, although the origin of the enhancement of ligand affinity by methoxy substituents was not deeply analyzed. Another interesting feature that can be observed from our calculated binding affinities is the additive character of the substituent effects: the higher the number of the substituents, the stronger their modulation of binding affinities. On the other hand, the specific position of the substituent in the aromatic ring does not lead to significant differences in the stability of both families of chelators (Table 2). These latter findings are in agreement with those reported in the literature, considering the stability constants of differently substituted (EWGs or EDGs) salicylic acids.[40,41]

In order to rationalize the opposite behavior of the two different types of substituents and to obtain a more detailed picture about the change in the electronic structure of these complexes, we proceeded to characterize the nature of the Al–O interactions by means of the QTAIM theory and Energy Decomposition Analysis (EDA).

Chemical bond analysis of Al–chelator interactions

QTAIM analysis suggests a mainly ionic interaction but with a sizeable covalent degree. Results of QTAIM topological analyses of the Al–O bond critical points (BCPs) for all 1 : 1 complexes are shown in the ESI Table S6.† The values of the electron density at all Al–O bond critical points, $\rho(r_{BCP})$, are rather small; such a situation has been reported in the literature as a typical feature for metal-containing systems.[65–67] Interestingly, there is very good correlation between $\rho(r_{BCP})$ and binding affinities (ΔG_{aq}^{comp}): the higher the value of $\rho(r_{BCP})$, the stronger the affinity (see ESI Fig. S3†). In addition, we find positive values of $\nabla^2\rho(r_{BCP})$, and small but negative values of the energy densities at the bond critical points $H(r_{BCP})$, consistently for all Al–O BCPs. Positive values of $\nabla^2\rho(r_{BCP})$ and $H(r_{BCP})$ are indicative of closed-shell interactions (*i.e.* ionic or electrostatic bonds), while negative values for both quantities indicate the presence of shared (covalent) interactions. The mixed situation present in our results, previously reported for bonds involving metals,[65] suggests that, although the Al–O bonds are mainly of ionic nature, there is also a small degree of covalency that could play a significant role. It is worth emphasizing that also both the Laplacians and the energy densities at all Al–O BCPs show a strong correlation with binding energies (ESI Fig. S4 and S5,† respectively). To further investigate these findings, we decided to calculate the delocalization indices (D.I.) for all the Al–O bonds. These indices are quantities integrated in the whole volumes of the respective atom basins, and therefore they give a more global and reliable picture of a bond inter-

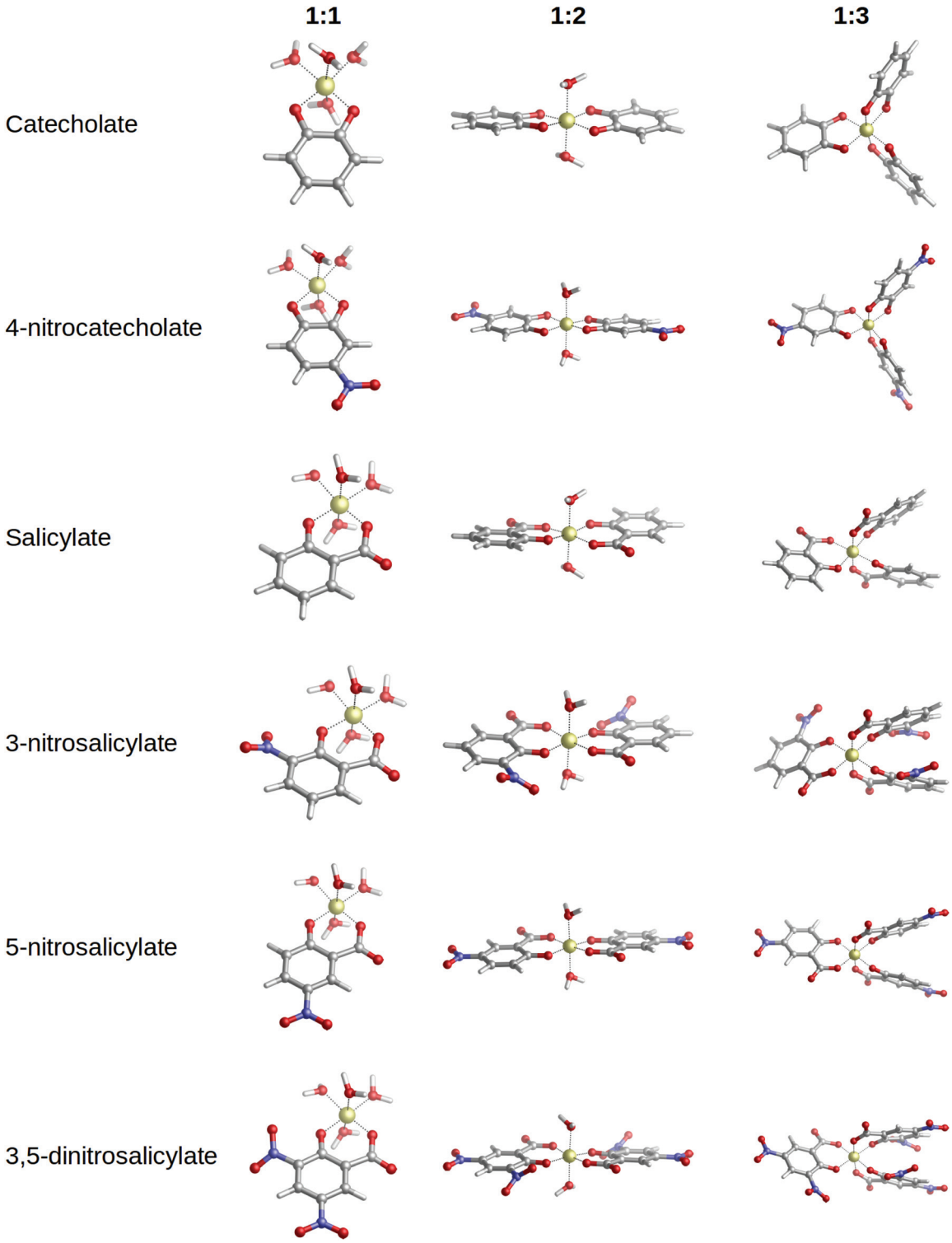

Fig. 4 Optimized geometries of 1 : 1, 1 : 2 and 1 : 3 Al(III)–chelator complexes used to validate the theoretical protocol: catechol, 4-nitrocatechol, salicylic acid, 3-nitrosalicylic acid, 5-nitrosalicylic acid, 3,5-dinitrosalicylic acid.

action than the analysis based on the properties of a single point in space like the bond critical point.

Delocalization indices show a strong correlation *versus* binding affinities. D.I. for all Al–O bonds are shown in the ESI Table S7,† along with the localization indices of aluminum. In Fig. 6, we represent ΔH_{aq}^{comp} *versus* the sum of the two Al–O delocalization indices for each complex ($D.I._{Al-O}$). The differences in Al–O bond delocalization indices among the various

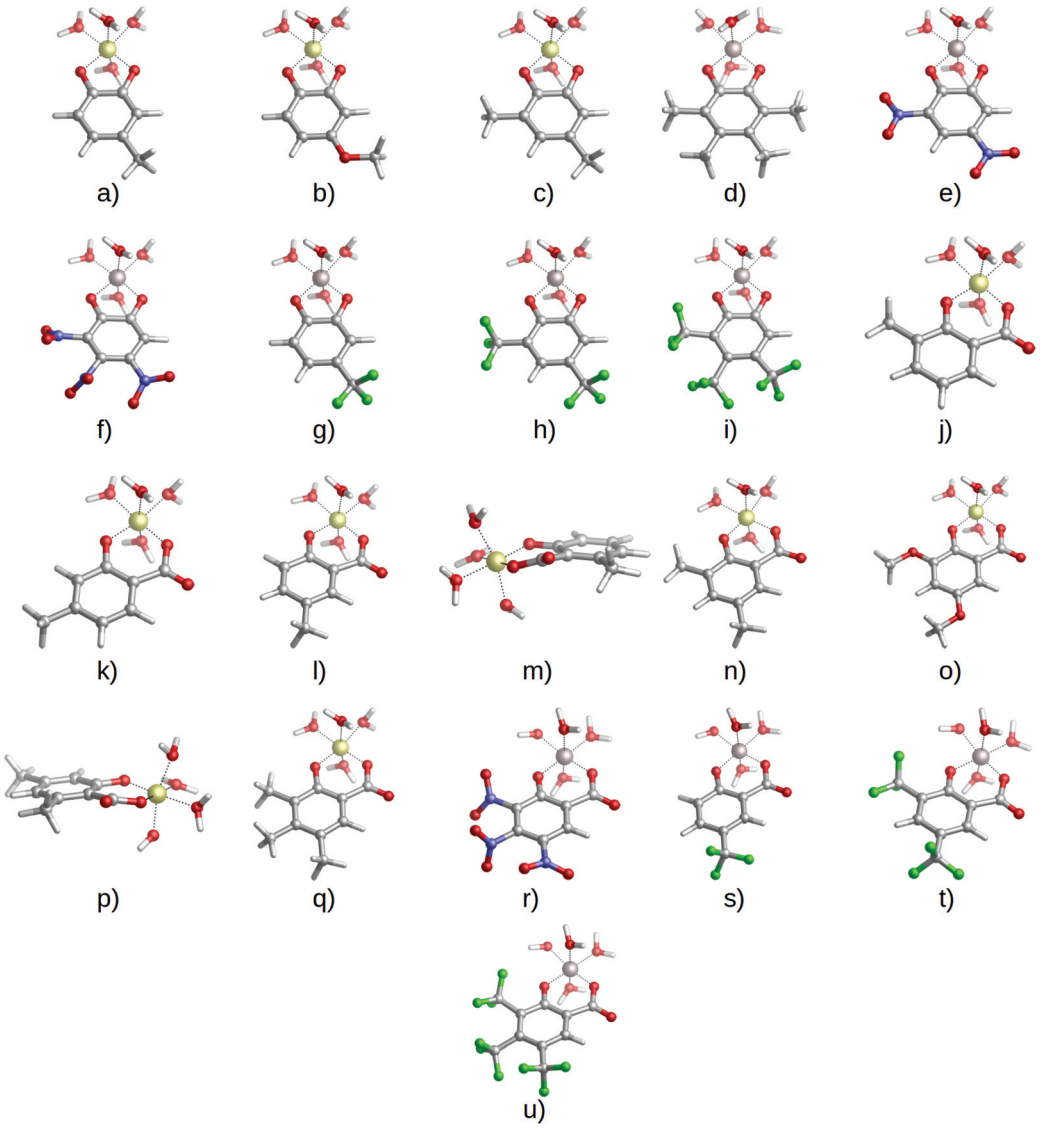

Fig. 5 Optimized geometries of 1 : 1 complexes between aluminum and catecholates or salicylates bearing the four different substituents: (a) 4-methylcatecholate, (b) 4-methoxycatecholate, (c) 4,6-dimethylcatecholate, (d) 3,4,5,6-tetramethylcatecholate, (e) 4,6-dinitrocatecholate, (f) 4,5,6-trinitrocatecholate, (g) 4-trifluoromethylcatecholate, (h) 4,6-trifluoromethylcatecholate, (i) 4,5,6-trifluoromethylcatecholate, (j) 3-methylsalicylate, (k) 4-methylsalicylate, (l) 5-methylsalicylate, (m) 6-methylsalicylate, (n) 3,5-dimethylsalicylate, (o) 3.5-dimethoxysalicylate, (p) 4,6-dimethylsalicylate, (q) 3,4,5-trimethylsalicylate, (r) 3,4,5-trinitrosalicylate, (s) 5-trifluoromethylsalicylate, (t) 3,5-trifluoromethylsalicylate, and (u) 3,4,5-trifluoromethylsalicyate.

complexes are small. Nevertheless, there is a clear correlation between the values of these delocalization indices and the binding affinities (see Fig. 6), finding a remarkable linear correlation between ΔH_{aq}^{comp} and D.I.$_{Al-O}$, with a value of the correlation coefficient (r) of 0.9854 for salicylates (16 compounds), 0.9926 for catecholates (11 compounds), and 0.9884 for the whole dataset of 27 compounds. Since D.I. are a measure of the number of electron pairs shared between two atoms, they have been related to the covalent character of a given bond.[68] Our results point to a clear modulation of the DI_{AlO} by the opposite effect of EDGs and EWGs, confirming our previous findings of a small but important degree of covalency in these mainly electrostatic interactions. The overall picture provides a clear rationalization of the effect of substituents: EDGs donate electron density to the aromatic ring, which in turn increase the covalency of the Al–O bonds, as can be seen by larger values of D.I.$_{Al-O}$, higher $\rho(r_{BCP})$ and more negative $H(r_{BCP})$ of the Al–O bonds (Fig. 6, S4, S5 and Tables S3 and S7†). On the other hand, EWGs take electron density away from the aromatic ring, leading to weaker Al–O interactions with lower D.I.$_{Al-O}$ values, lower $\rho(r_{BCP})$ and less negative $H(r_{BCP})$. In summary, QTAIM topological analysis and D.I. suggest that there is a degree of covalency in the Al–O interactions, modulated by the effect of substituents, which correlates with both theoretical (ΔG_{aq}^{comp}, ΔH_{aq}^{comp}) and experimental ($\log\beta$ when available) binding affinities. It is also important to note that

Table 2 Binding enthalpies (ΔH_{aq}^{comp}) and free energies (ΔG_{aq}^{comp}) in kcal mol^{-1} computed for 1 : 1 complexes (compounds are shown in Fig. 1) considering the whole dataset of compounds bearing different substituents

Ligand	ΔH_{aq}^{comp}	ΔG_{aq}^{comp}
Catecholates		
Catecholate	−88.4	−91.4
Electron withdrawing groups		
4-Nitrocatecholate	−71.6	−75.8
4,6-Dinitrocatecholate	−62.0	−65.9
4,5,6-Trinitrocatecholate	−52.8	−56.4
4-Trifluoromethylcatecholate	−81.4	−87.1
4,6-Trifluoromethylcatecholate	−75.5	−78.6
4,5,6-Trifluoromethylcatecholate	−70.1	−74.0
Electron donating groups		
4-Methylcatecholate	−89.5	−93.3
4,6-Dimethylcatecholate	−91.6	−95.4
3,4,5,6-Tetramethylcatecholate	−97.2	−101.2
4-Methoxycatecholate	−89.6	−92.8
Salicylates		
Salicylate	−76.9	−78.7
Electron withdrawing groups		
3-Nitrosalicylate	−64.2	−66.7
5-Nitrosalicylate	−63.3	−65.4
3,5-Dinitrosalicylate	−57.1	−55.0
3,4,5-Trinitrosalicylate	−50.5	−52.4
5-Trifluoromethylsalicylate	−70.3	−75.3
3,5-Trifluoromethylsalicylate	−65.5	−67.6
3,4,5-Trifluoromethylsalicylate	−61.8	−64.2
Electron donating groups		
3-Methylsalicylate	−79.2	−82.5
4-Methylsalicylate	−79.3	−82.3
5-Methylsalicylate	−79.3	−82.9
6-Methylsalicylate	−74.9	−77.2
3,5-Dimethylsalicylate	−80.7	−83.6
4,6-Dimethylsalicylate	−76.4	−79.4
3,4,5-Trimethylsalicilate	−82.0	−85.3
3,5-Dimethoxysalicylate	−79.5	−82.3

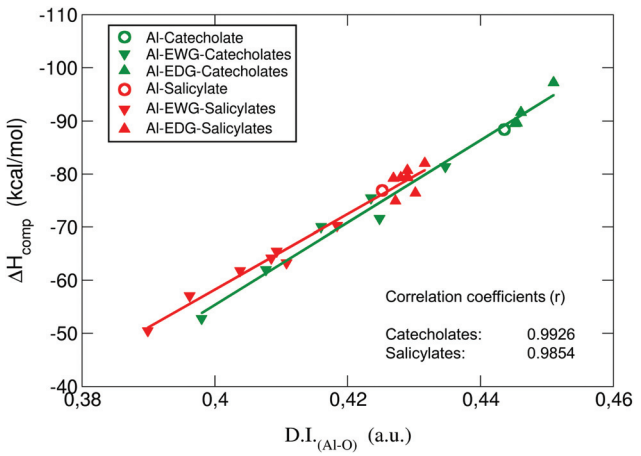

Fig. 6 Binding enthalpies ΔH_{aq}^{comp} in kcal mol^{-1} *versus* the sum of the two Al–O delocalization indices ($D.I._{Al-O}$) in a.u. for all complexes.

values of aluminum localization indices (average number of electrons localized on a given atom) are stable among different compounds, suggesting that no charge transfer takes place in these aluminum–chelator complexes.

Finally, we would also like to highlight the effect that substituents have in the modulation of atomic charges at the oxygen atoms coordinated to aluminum. In general, methyl and methoxy groups tend to increase the negative charges at those oxygen atoms, whereas the presence of nitro and trifluoromethyl groups lead to lower negative charges in both families (see the ESI Table S7†). Quite interestingly, high electron delocalizations from the lone pairs of the two oxygens to the 3s and 3p orbitals of aluminum were assessed by means of the Natural Bond Orbital approach. According to these latter findings, we can rationalize such small covalent character as a dative interaction between the two oxygen donors and the formally empty orbitals of the metal.

To further investigate the relative contributions of the electrostatic and covalent components of these Al–O bonds, we performed the Energy Decomposition Analysis (EDA) of all compounds.

Energy decomposition analysis confirms a mainly ionic bond with a significant covalent character that modulates the binding affinity. In the ESI Table S8,† we can find the values of the Energy Decomposition Analysis terms calculated at the B3LYP-D3(BJ)/ET-QZ3P-1DIFFUSE level of theory in the gas phase (see specific computational details in the ESI†). In Fig. 7, we represent the values of binding enthalpies *versus* the total EDA interaction energies (ΔE_{int}), and its electrostatic (ΔE_{elstat}) and orbital interaction (ΔE_{oi}) components. First, we have to remark that there is a good linear correlation (r = 0.9727, salicylates and r = 0.9841, catecholates) between the total interaction energies calculated with EDA and ΔH_{aq}^{comp}, noting the adequacy of using the EDA analysis to understand the origin of the different affinities of the chelators towards aluminum. The decomposition of interaction energies into electrostatic and orbital interaction (which accounts for the covalent character) terms points to mainly electrostatic interactions, and, in agreement with the previous QTAIM analysis, there is a sizable contribution from orbital interaction terms (between 27% and 37%). In general, the percentage of covalency is higher for catecholates than for salicylates (Fig. 7 and ESI Table S8†), and EWGs tend to decrease the degree of covalency of these interactions, whereas EDGs increase it. However, it is important to take into account that such calculations were performed in the gas phase; therefore, environmental effects (*i.e.* implicit solvent) are expected to alter the degree of the covalent character. Interestingly, although ΔE_{elstat} is significantly larger than ΔE_{oi} in all compounds, it is only the latter that correlates with the binding enthalpies (see Fig. 7). The linear regression of ΔH_{aq}^{comp} *versus* ΔE_{oi} shows a correlation coefficient of 0.8964 for salicylates (16 compounds) and 0.9366 for catecholates (11 compounds), and 0.9185 if we consider the whole dataset of 27 compounds. Conversely, there is no correlation between ΔH_{aq}^{comp} and ΔE_{elstat}, and even though salicylates have on average larger electrostatic interaction energy

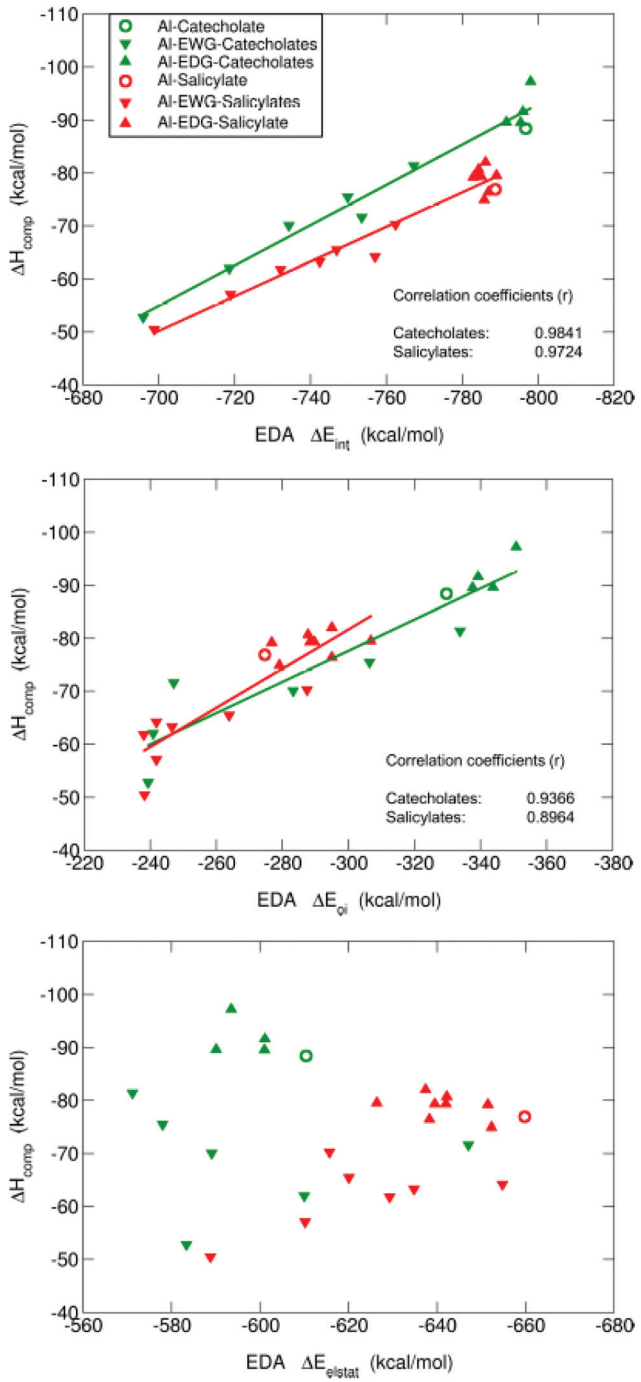

Fig. 7 Representation of the binding enthalpies (ΔH_{aq}^{comp}) *versus* three components of the Energy Decomposition Analysis: (i) total interaction energies (top diagram), (ii) orbital interaction term (middle diagram) and (iii) electrostatic energy term (bottom diagram) for all the 11 aluminum–catecholate and 16 aluminum–salicylate compounds. All energies are in kcal mol^{-1}.

than catecholates, they have lower affinity for aluminum. The other two terms of the EDA, ΔE_{Pauli} and ΔE_{disp} (see Table S8†), don't show significant variations and therefore don't have a direct influence on the overall behaviour of these compounds.

In summary, in agreement with QTAIM analysis, the tuning of the covalency of the Al–O bonds by the different EWG/EDG substituents modulates the differential affinities towards aluminum shown by these chelators. In this sense, the introduction of nitro and trifluoromethyl groups in the catecholate and salicylate rings leads to smaller absolute values of ΔE_{oi}, and this decrease is significantly larger for the former than for the latter. On the other hand, methyl and methoxy substituents lead to larger orbital interactions.

The role of aromaticity

The aromatic character of the ligands could be important to transmit the substituent effects. As can be seen in Fig. 1, the four substituents provide different effects: nitro is an EWG by both inductive and resonance effects, trifluoromethyl is an EWG only by inductive effect, methoxy shows opposite effects that partially compensate, (electron withdrawing by induction and electron donating by resonance), and finally methyl is an EDG only by the inductive effect. Therefore, we chose to investigate how the aromaticity of the ligands changes upon aluminum binding and introduction of substituents. We investigate the aromatic character of all complexes according to the I_{ring} and MCI aromatic descriptors[69] (see specific computational details in the ESI and Table S9†). Both give similar trends and we will focus our discussion on I_{ring} indices. Benzene is used as reference for an aromatic compound, while cyclohexane for a non-aromatic one. As expected, both catechol and salicylic acid show lower aromatic characters than the pure benzene ring. Upon deprotonation, both catecholate and salicylate display a sizable reduction of the aromatic character to 0.0235 and 0.0306 a.u., respectively. Notice, however, that upon aluminum binding the values are restored to 0.0345 and 0.0351 a.u. Thus, in terms of aromaticity, the interaction with aluminum recovers the values obtained for the original protonated catechol and salicylic acid. For the rest of the discussion, we will focus on Al-bound complexes, taking as reference the corresponding unsubstituted Al-catecholate/salicylate complex.

In both families of chelators, the addition of substituents, independently of the electron donating/withdrawing nature, decreases the aromatic character of the complexes. Moreover, such a decrease in aromaticity follows a clear trend depending on the number of substituents that are added, so that the higher the number of substituents, the lower the aromatic character of the corresponding complex. Interestingly, substituents with a mechanism of action mediated by resonance (nitro and methoxy) show a larger decrease of aromaticity than those that work through inductive effect (methyl and trifluoromethyl). The lowest aromatic character is observed for trinitro-substituted compounds (4,5,6-trinitrocatecholate and 3,4,5-trinitrosalicylate), with values of 0.0207 and 0.0249 a.u., respectively. Regarding the electron-donating substituents, methoxy leads to lower aromaticity indices than methyl, because in aromatic molecules resonance effect dominates over inductive effect and methoxy has an overall electron donating behavior.

One may ask, as partially hypothesized by Dean *et al.*[42] for similar pyridine-based aluminum chelators, whether the aromatic character of a chelating agent is one of the main factors contributing to the different stabilities of the Al–chelator complexes. Clearly, our calculations point to a negative answer. Both EWGs and EDGs decrease the aromatic character of the compounds, but in the latter case there is an increase in the affinity towards aluminum. Thus, aromaticity does not play a direct role in the stabilization of these aluminum–chelator complexes.

Nevertheless, the role of aromaticity is critical to modulate the mechanism of action of the substituents through resonance. In order to analyze this aspect, we calculated the binding energies of a series of non-aromatic 4-*R*-1,2-dihydroxy-cyclohexanes (see Fig. 8), and evaluated the changes in the binding affinities towards aluminum caused by the introduction of the four substituents listed in Fig. 1. The results are summarized in Fig. 8, where we depict the relative binding energies $\Delta\Delta G_{aq}^{comp}$ of each complex with respect to the unsubstituted chelator in each case. We can see important differences in $\Delta\Delta G_{aq}^{comp}$ between aromatic and non-aromatic compounds: while in the case of non-aromatic chelators the range of $\Delta\Delta G_{aq}^{comp}$ expands from −0.6 kcal mol^{-1} to 6.4 kcal mol^{-1}, in the case of the aromatic catecholates $\Delta\Delta G_{aq}^{comp}$ expands to a much larger range, from −1.9 kcal mol^{-1} to 15.7 kcal mol^{-1}. This is indicative of a larger sensitivity of aromatic chelators towards substituent effects. Notice for instance, the large increase in $\Delta\Delta G_{aq}^{comp}$ when considering the nitro group, 6.4 kcal mol^{-1} (non-aromatic chelator) *versus* 15.7 kcal mol^{-1} (aromatic chelator); clearly, this difference demonstrates that when the resonance transmission mechanism of the substituent is absent, the nitro group loses some of its electron-withdrawing character, partially maintained by the inductive-based one. Methoxy is a very significant case: while in the case of the aromatic chelator –OCH_3 leads to stabilizing effects (−1.4 kcal mol^{-1}), in the case of the non-aromatic compound it leads to a destabilizing effect (0.8 kcal mol^{-1}). This is due to the fact that –OCH_3 acts as an EDG by resonance, but as an EWG by inductive effect. Accordingly, when resonance is absent like in 4-methoxy-1,2-dihydroxy-cyclohexane, the inductive-based electron withdrawing mechanism is the only one working.

In summary, although the introduction of electron donating/withdrawing substituents in both catecholate and salicylate families of chelators reduce the aromaticity of the compounds, the complexes still retain enough aromatic character to permit the transmission of substituent effects by a combination of both resonance and inductive mechanisms. This is a key factor in tuning the covalent character of the Al–O interactions.

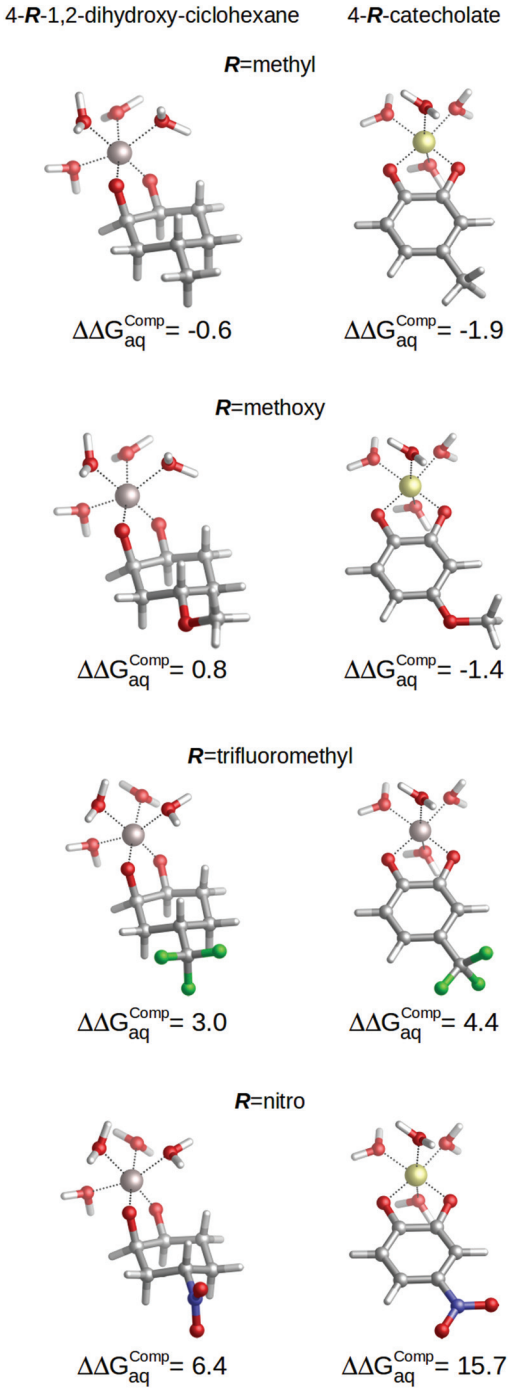

Fig. 8 Relative binding energies ($\Delta\Delta G_{aq}^{Comp}$) of non-aromatic (4-*R*-1,2-dihydroxy-cyclohexane) and aromatic (4-*R*-catecholate) chelators calculated with respect to their unsubstituted counterparts. *R* can be methyl, methoxy, nitro or trifluoromethyl. All energies are in kcal mol^{-1}.

Proton and aluminum ion competition

So far, we have not considered the possible competition between Al(III) and proton(s) for ligand binding. In other words, the overall performance of a chelator at a given pH will be dictated not only by the stability of the corresponding aluminum–ligand complex, but also by the deprotonation capacity of a ligand at a certain pH. As a result, the experimental trends in $\log\beta$ and p[Al] to characterize the performance of a given chelator can differ[62,64] (see Table 1). For instance, catechol shows a p[Al] value of 10.1, and the introduction of a nitro electron-withdrawing group raises this value

up to 14.2, indicating better chelation properties.[40] However, as we have seen, 4-nitro-catecholate shows a lower $\log\beta$ value than the unsubstituted catecholate (see Table 1). Conversely, in the case of salicylic acids, Nurchi *et al.*[41] reported that methoxy-substituted salicylic acids (an overall electron-donating group) show significant higher p[Al] values (9.6/10.2 for *ortho*/*para* methoxy-salicylic acid) than the unsubstituted one (8.2), while the introduction of a nitro group provokes only a moderate variation of p[Al], (8.4/8.7 for *ortho*/*para* nitro-salicylic acid). What is the reason for these differential trends between salicylic acids and catechols, and between $\log\beta$ and p[Al] in catechols? We have to take into account that whereas $\log\beta$ is a measure of the stability of the complex with respect to the dissociation of unprotonated ligands, p[Al] takes into account additional factors, like proton/metal ion competition. Another important difference is that $\log\beta$ is specific for each stoichiometry, while different stoichiometries and denticities contribute to a given value of p[Al].[28,64]

In order to account for proton/metal ion competition in our calculations, we have evaluated the relative proton affinities of the different ligands, and combine them with the relative aluminum affinities. The procedure is as follows: we evaluate the relative proton affinities of the ligands with a given functional group with respect to the unsubstituted catechol and salicylic acid, by the estimation of the following $\Delta\Delta G^{nH}(\mathrm{L_{subs}}^{-2})$ reaction energy:

$$\mathrm{Cat}^{2H,0} + \mathrm{Cat_{subs}}^{-2} \xrightarrow{\Delta\Delta G^{2H}(L_{subs}{}^{-2})} \mathrm{Cat_{subs}}^{2H,0} + \mathrm{Cat}^{-2} \quad (4)$$

$$\mathrm{Sal}^{1H,-1} + \mathrm{Sal_{subs}}^{-2} \xrightarrow{\Delta\Delta G^{1H}(\mathrm{L_{subs}}^{-2})} \mathrm{Sal_{subs}}^{1H,-1} + \mathrm{Sal}^{-2} \quad (5)$$

As one can see in these equations, there is an important difference between catechols and salicylic acids. The pK_a values of catechols (see Table 3 and ref. 40) are such that at neutral pH both chelating positions are likely to be protonated and, therefore, Al(III) binding has to compete with the removal of two protons from the ligand. However, the first pK_{a1} of salicylic acid is so low (see Table 3 and ref. 40 and 41) that at neutral pH the carboxylic group is undoubtedly unprotonated; accordingly, the binding of the aluminum ion only involves the removal of the hydroxyl proton. Besides, we define a relative aluminum affinity of a given ligand in each family of compounds with respect to the unsubstituted ligand, using the ΔG_{aq}^{comp} values of Table 2, namely:

$$\mathrm{Al\text{–}Lig}^{-2} + \mathrm{Lig_{subs}}^{-2} \xrightarrow{\Delta\Delta G^{Al}(\mathrm{L_{subs}}^{-2})} \mathrm{Al\text{–}Lig_{subs}}^{-2} + \mathrm{Lig}^{-2} \quad (6)$$

$$\Delta\Delta G^{\mathrm{Al}}(\mathrm{L_{subs}}^{-2}) = \Delta G_{aq}^{comp}(\mathrm{Al\text{–}L_{subs}}^{-2}) - \Delta G_{aq}^{comp}(\mathrm{Al\text{–}L}^{-2}) \quad (7)$$

with Lig = catecholate, salicylate. Combining the relative proton/aluminum ion affinities, we can estimate a value for the relative Al(III) affinity of a ligand that takes into account proton/metal ion competition, namely,

$$\Delta\Delta G^{\mathrm{Al}}(\mathrm{Al\text{–}L_{subs}}^{nH}) = \Delta\Delta G^{\mathrm{Al}}(\mathrm{Al\text{–}L_{subs}}^{-2}) - \Delta\Delta G^{nH}(\mathrm{L_{subs}}^{-2}) \quad (8)$$

Table 3 Relative proton affinities with respect to catechols and salicylic acids in kcal mol^{-1}. Experimental protonation constants are taken from ref. 40

Ligand	$\Delta\Delta H_{subs}{}^{2H}$	$\Delta\Delta G_{subs}{}^{2H}$	pK_{a1} (exp)	pK_{a2} (exp)
$\mathrm{Cat}^{2H,0} + \mathrm{Cat_{subs}}^{-2} \rightarrow \mathrm{Cat_{subs}}^{2H,0} + \mathrm{Cat}^{-2}$				
Catechol	0.0	0.0	9.2	14.3
Electron withdrawing groups				
4-Nitrocatechol	21.3	20.8	6.6	10.7
4,6-Dinitrocatechol	36.0	36.0		
4,5,6-Trinitrocatechol	47.6	46.9		
4-Trifluoromethylcatechol	9.3	6.2		
4,6-Trifluoromethylcatechol	18.7	19.0		
4,5,6-Trifluoromethylcatechol	26.4	26.0		
Electron donating groups				
4-Methylcatechol	−1.6	−3.0		
4,6-Dimethylcatechol	−3.9	−4.8		
3,4,5,6-Tetramethylcatechol	−9.1	−10.1		
4-Methoxycatechol	−1.6	−1.6		
$\mathrm{Sal}^{1H,-1} + \mathrm{Sal_{subs}}^{-2} \rightarrow \mathrm{Sal_{subs}}^{1H,-1} + \mathrm{Sal}^{-2}$				
Salicylic acid	0.0	0.0	3.1	13.6
Electron withdrawing groups				
3-Nitrosalicylic acid	10.8	10.5	1.5	9.9
5-Nitrosalicylic acid	11.4	11.8	1.7	10.0
3,5-Dinitrosalicylic acid	16.0	16.3	−0.1	7.0
3,4,5-Trinitrosalicylic acid	18.9	18.9		
5-Trifluoromethylsalicylic acid	5.2	2.9		
3,5-Trifluoromethylsalicylic acid	9.7	9.4		
3,4,5-Trifluoromethylsalicylic acid	12.7	12.6		
Electron donating groups				
3-Methylsalicylic acid	−0.9	−1.1		
4-Methylsalicylic acid	−1.0	−1.3		
5-Methylsalicylic acid	−1.1	−0.7		
6-Methylsalicylic acid	2.5	1.5		
3,5-Dimethylsalicylic acid	−2.4	−2.7		
4,6-Dimethylsalicylic acid	1.5	1.4		
3,4,5-Trimethylsalicylic acid	−3.4	−3.7		
3,5-Dimethoxysalicylic acid	−2.1	−1.3		

with n = 2 for catechols and n = 1 for salicylic acids. The results for $\Delta\Delta G^{nH}(\mathrm{L_{subs}}^{-2})$ can be found in Table 3 and Fig. 9-A, and the results for $\Delta\Delta G^{\mathrm{Al}}(\mathrm{Al} - \mathrm{L_{subs}}^{nH})$ are also plotted in Fig. 9-B.

As one can see in Fig. 9A, EDGs lie at the top-right side of the diagram, whereas EWGs are at the bottom-left side, manifesting that those ligands that have the largest affinities for aluminum also display the largest affinities for protons. This is the case for both catechols and salicylic acids, but with an important difference. Catechols span a wider range of relative proton affinities than salicylic acids, a fact mainly attributed to the fact that two protons are removed in catechol and only one in salicylic acids. In order to estimate the aluminum relative binding affinity in the presence of protonated ligands (Fig. 9B), we have to combine these two relative proton/aluminum affinities according to eqn (8), to yield $\Delta\Delta G^{\mathrm{Al}}(\mathrm{Al\text{–}L_{subs}}^{2H})$ (displayed in the y-axis of Fig. 9B). Our data clearly show an inverse trend between $\Delta\Delta G^{\mathrm{Al}}(\mathrm{Al\text{–}L_{subs}}^{2H})$ and $\Delta\Delta G^{\mathrm{Al}}(\mathrm{Al\text{–}L_{subs}}^{-2})$ for catechols, but not for salicylic acids. Our results for catechols suggest that the introduction of EWGs leads to a better Al(III) chelation performance upon competition with the removal of two protons, and this corresponds to the previously

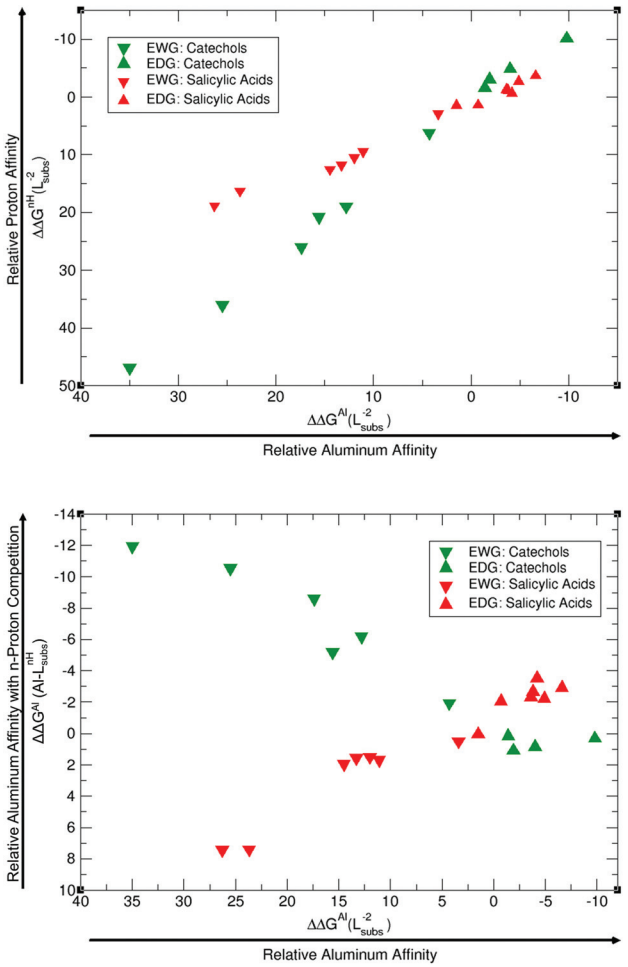

Fig. 9 Proton *versus* aluminum competition analysed as: (a) $\Delta\Delta G^{nH}(L_{subs}{}^{-2})$ *vs.* $\Delta\Delta G^{Al}(L_{subs}{}^{-2})$ (top diagram) and (b) $\Delta\Delta G^{Al}(Al{-}L_{subs}{}^{nH})$ *vs.* $\Delta\Delta G^{Al}(L_{subs}{}^{-2})$ (bottom diagram). Terms defined in the body text. All relative affinities are in kcal mol^{-1}.

described experimental increase of *p*[Al] with nitro-substitution (Tables 1 and 3). In the case of salicylic acids, since we are only removing one proton upon aluminum binding, relative aluminum affinity is still the overall leading factor in chelator binding, and now it is the introduction of an EDG that clearly improves the performance of the chelator. This is again in agreement with the clear increase in the experimental *p*[Al] of salicylic acids upon the introduction of methoxy groups.[41] In summary, our results demonstrate that in the competition between aluminum binding and deprotonation, the latter factor dominates when the binding of Al(III) requires the removal of two protons from the ligand, whereas the former is dominant if only one proton has to be removed, in agreement with the experimental results for catechols and salicylic acids, respectively.[40,41]

To complete our analysis, we provide a possible explanation of how the introduction of EWGs (*i.e.* nitro) in salicylic acids lead to similar albeit a bit higher *p*[Al] values.[40] Our data for 1 : 1 complexes show a moderate decrease in $\Delta\Delta G^{Al}(Al{-}L_{subs}{}^{1H})$ for both 3- and 5-nitro-substitution (namely 1.5 kcal mol^{-1}), which in principle should point to a lower value of *p*[Al]. One aspect should be remarked in this regard: the experimental values of *p*[Al] don't take into account only 1 : 1 aluminum–ligand stoichiometry, but different stoichiometrical complexes like 1 : 2 and 1 : 3. Therefore, we recalculated the differential binding free energies for 1 : 2 and 1 : 3 stoichiometries of the single nitro-substituted salicylic acids of Table 1, namely,

$$\Delta\Delta G^{Al}(Al{-}[L_{subs}{}^{1H}]_n) = \Delta\Delta G^{Al}(Al{-}[L_{subs}{}^{-2}]_n) + n \times \Delta\Delta G_{subs}{}^{1H} \quad (9)$$

where *n* is the number of ligands bound to aluminum. The results are as follows: for 1 : 1 complexes, we obtain values for $\Delta\Delta G^{Al}(Al{-}[L_{subs}{}^{1H}]_1)$ of 1.5 kcal mol^{-1} (3-nitro), 1.5 kcal mol^{-1} (5-nitro); for 1 : 2 complexes: 1.3 kcal mol^{-1} (3-nitro), −0.9 kcal mol^{-1} (5-nitro); finally, for 1 : 3 complexes, we found −9.8 kcal mol^{-1} (3-nitro), −9.6 kcal mol^{-1} (5-nitro). Thus, we can observe how the stoichiometry is an additional contributing factor in the modulation of the aluminum ion/proton competition for ligand binding, with higher stoichiometries favoring those substituents that lead to a more favorable deprotonation (*i.e.* EWGs), albeit lower interaction with aluminum itself. The overall result is that, for 1 : 3 complexes, the introduction of EWGs promotes their chelation to aluminum because of the lower protonation energies (*i.e.* lower protonation constants, Table 3), and would lead to higher *p*[Al] values; the case of 1 : 2 complexes lies in between 1 : 1 and 1 : 3-related behavior. The fact that the experimental data point only to a moderate increase in *p*[Al] upon nitro introduction in salicylic acids suggests that different stoichiometries with opposite effects are contributing to these values, and thus there is a partial cancelation and compensation of their effects. Finally, it is important to mention that both families of compounds, when protonated, form an intramolecular hydrogen bond between the two phenolates (catechol) and phenolate and carboxylate (salicylic acid), which is a further factor contributing to the modulation of the aluminum/proton competition.

Tuning the molecule: the role of substituents

The present paper provides the most complete and thorough theoretical study of the interaction of aluminum with catechols and salicylic acids chelating agents done so far. We have identified and rationalized important factors affecting ligand binding to aluminum, which are crucial to design new chelators of increased affinity. Namely, we have characterized the strength of the aluminum–ligand interactions, interpreted the binding strengths in terms of the electrostatic/covalent nature of the Al–O bonds, unveiled the role played by the aromaticity of these chelators, rationalized the modulation of the stability through addition of substituents and, finally, determined how aluminum/proton competition affects the overall activity of a chelator.

In this sense, our calculations demonstrate that although the bond is mainly electrostatic in nature, as it corresponds to a hard metal, the fine tuning of the stability in both families of chelators is mediated through the modulation of the covalent character of the Al–O bonds. This covalent character can be classified as a dative bond from the lone pair of the oxygens to the 3s, 3p valence shell of Al(III). The increase in the dative Al–O bond character through the introduction of EDGs leads to complexes of higher stability, whereas EWGs lead to complexes of lower stability, in agreement with the experimental trends of $\log\beta$ (Table 1). Such a picture is also coherent with the Pearson's Hard and Soft Acids and Bases (HSAB) principle;[70] indeed, the two phenolate groups of catechol are harder Lewis bases than the carboxylate one of salicylic acid, because of the intrinsic resonance of the COO^- moiety, and therefore the former are expected to show higher affinity for hard Lewis acids such as Al(III). This is quite interesting considering that the salicylate family shows, overall, a higher electrostatic interaction (three negatively charged oxygens) than the catecholate family,[61] as shown by EDA results (see Table S8†); nevertheless, the catecholate family has a higher affinity for the trivalent metal, a fact that can be related to the more covalent Al–O bond as revealed by both QTAIM and EDA results and summarized in Fig. S6.†

We have also determined the role that the aromatic nature of these two families of chelators plays in the metal–ligand complexes. Aromaticity is only slightly affected upon aluminum binding, being more sensible to the introduction of EDG/EWG substituents in the ring. In both salicylates and catecholates, the introduction of both electron donating/withdrawing substituents leads to a lower aromatic character. Nevertheless, a significant degree of aromaticity is maintained in all complexes, which is pivotal to modulate and transmit some of the resonance-based substituent effects.

We should remark that, although the covalent character is the main driving factor in the modulation of the affinity toward aluminum for these two families of chelators, other factors can also affect the observed stability. For instance, in some of the complexes we found steric hindrances that put them out of the general trend in binding energy (see Table 2). Indeed, 6-methylsalicylate has a lower stability when compared with unsubstituted salicylic acid, despite the presence of an EDG, which should enhance its binding affinity. The optimized geometry for that compound shows that the six-membered ring formed by aluminum, the carboxylate and the enolate groups is slightly distorted from full planarity (by 16.8° and 20.9°), suggesting a steric repulsion between methyl at the 6 position and the carboxylate group (compound 'm' in Fig. 5). Such a situation leads to a decrease in binding affinity (Table 2). Moreover, if we consider 4,6-dimethylsalicylate (compound 'p' in Fig. 5), we can see that the addition of a second methyl in position 4 partially recovers the stability and planarity of the complex (12.6° and 15.6°) when compared with salicylate (Table 2), because of the electron donating effect that counterbalances the steric repulsion of the methyl in position 6. However, the recovered stability is still not as high as for another di-substituted compound like 3,5-dimethylsalicylate (0.1° and 0.1°), where no steric effects are present (compound 'n' in Fig. 5). This situation was also hypothesized by Dean *et al.*[43] for similar compounds. It is clear that, when considering new strategies toward the improvement and design of new Al(III) chelating agents, one should carefully consider possible repulsive phenomena. Regarding proton/aluminum ion competition, we have been able to reproduce the inverse trends in ligand affinity when comparing $\log\beta$ and p[Al] values for catechols (Table 1), and to explain how the introduction of an electron withdrawing group in catechols, but electron donating group in salicylic acids, enhances the chelation properties of the ligands upon competition with protonation. Taking into account that the metal/proton competition for ligand binding is critical to determine the performance of a given ligand in chelation therapy, as established by Hider *et al.*,[62] complex stability is also important in order to compete with other endogenous ligands (like citrate) in an open biological environment.[71] Moreover, if the stability of the Al(III)–chelator complex is too weak, then the metal may prefer to form the very stable $[Al(OH)_4]^-$ hydroxo complex.[61,72] We have found that those substituents that favor aluminum binding (in terms of $\log\beta$) also favor protonation.[40,41,62] The overall effect is a balance between the Al(III)–ligand complex stability and the competition with H^+. In this sense, EWGs, by lowering the affinity toward aluminum, also favor deprotonation (by lowering the protonation constants of the ligand), and this latter factor is the dominant one at a pH in which aluminum competes with two protons for ligand binding. Conversely, when only one proton has to be removed, like in salicylic acids at weakly acidic or neutral pH, the nature of the dominant factor shifts to aluminum complex stability. Other factors such as stoichiometry of the complex can also contribute to the proton/aluminum ion competition toward a given ligand. Our results suggest that higher stoichiometries favor deprotonation as a leading factor in the overall performance of a given chelator.

Conclusions

In the present work, we have developed, validated and applied a state-of-the-art theoretical protocol suitable for the investigation of two families of bidentate Al(III) chelating agents (catechols and salicylic acids). Trends in binding affinities show very good agreement with respect to available experimental data. We have rationalized our results analyzing the nature of the Al–O bonds, finding that the covalent part of a mainly ionic Al–O interaction is the driving force in the fine-tuning of the stability of these complexes. Such a covalent character is modulated by the opposite effect of the substituents: methyl and methoxy groups increase this covalency, leading to higher affinities, whereas the nitro and trifluoromethy groups decrease the covalent component leading to lower binding affinities. We have also determined how the overall performance of a chelator depends critically on the metal/proton com-

petition toward ligand binding. In summary, the present work establishes a reliable and transferable theoretical protocol aimed to test the behavior of metal organic chelators, which would help in the future design and tuning of novel chelating agents of increased efficacy.

Conflicts of interest

There are no conflicts to declare.

Acknowledgements

This research has been funded by the Spanish MINECO/FEDER Projects CTQ2015-67608-P (X. L.), CTQ2014-52525-P (E. M.), EUIN2017-88605 (E. M.) and the Basque Country Consolidated Group Project No. IT588-13. The authors would like to thank the technical and human support provided by the SGI/IZO (SGIker) of the UPV/EHU. Financial support comes as well from the European Commission, Horizon 2020 Research and Innovation Programme (grant agreement N 642294 TCCM). This work received financial support from the European Union (FEDER funds POCI/01/0145/FEDER/007728) and National Funds (Fundação para a Ciência e Tecnologia and Ministério da Educação e Ciência–FCT/MEC) UID/MULTI/04378/2013, under the Partnership Agreement PT2020; NORTE-01-0145-FEDER-000024, supported by Norte Portugal Regional Operational Programme (NORTE 2020), under the PORTUGAL 2020 Partnership Agreement, through the European Regional Development Fund (ERDF).

References

1 C. Exley, *J. Inorg. Biochem.*, 2003, **97**, 1–7.
2 J. Beardmore, X. Lopez, J. I. Mujika and C. Exley, *Sci. Rep.*, 2016, **6**, 30913.
3 R. B. Martin, *Acc. Chem. Res.*, 1994, **27**, 204–210.
4 R. A. Yokel and P. J. McNamara, *Pharmacol. Toxicol.*, 2001, **88**, 159–167.
5 C. A. Shaw and L. Tomljenovic, *Immunol. Res.*, 2013, **56**, 304–316.
6 C. C. Willhite, N. A. Karyakina, R. A. Yokel, N. Yenugadhati, T. M. Wisniewski, I. M. F. Arnold, F. Momoli and D. Krewski, *Crit. Rev. Toxicol.*, 2014, **44**(Suppl 4), 1–80.
7 C. Exley, *Free Radical Biol. Med.*, 2004, **36**, 380–387.
8 J. I. Mujika, F. Ruipérez, I. Infante, J. M. Ugalde, C. Exley and X. Lopez, *J. Phys. Chem. A*, 2011, **115**, 6717–6723.
9 F. Ruipérez, J. I. Mujika, J. M. Ugalde, C. Exley and X. Lopez, *J. Inorg. Biochem.*, 2012, **117**, 118–123.
10 C. Exley, N. C. Price and J. D. Birchall, *J. Inorg. Biochem.*, 1994, **54**, 297–304.
11 S. J. Yang, J. W. Huh, J. E. Lee, S. Y. Choi, T. U. Kim and S. W. Cho, *Cell. Mol. Life Sci.*, 2003, **60**, 2538–2546.
12 J. I. Mujika, J. M. Ugalde and X. Lopez, *J. Phys. Chem. B*, 2014, **118**, 6680–6686.
13 P. Zatta, E. Lain and C. Cagnolini, *Eur. J. Biochem.*, 2000, **267**, 3049–3055.
14 J. Lemire, C. Auger, R. Mailloux and V. D. Appanna, *J. Neurosci. Res.*, 2014, **92**, 464–475.
15 J. Lemire, R. Mailloux, S. Puiseux-Dao and V. D. Appanna, *J. Neurosci. Res.*, 2009, **87**, 1474–1483.
16 R. J. Mailloux, R. Hamel and V. D. Appanna, *J. Biochem. Mol. Toxicol.*, 2006, **20**, 198–208.
17 E. Formoso, J. I. Mujika, S. J. Grabowski and X. Lopez, *J. Inorg. Biochem.*, 2015, **152**, 139–146.
18 V. Kumar and K. D. Gill, *Arch. Toxicol.*, 2009, **83**, 965–978.
19 I. Klatzo, H. Wisniewski and E. Streicher, *J. Neuropathol. Exp. Neurol.*, 1965, **24**, 187–199.
20 R. Grande-Aztatzi, J. M. Mercero and J. M. Ugalde, *Phys. Chem. Chem. Phys.*, 2016, **18**, 11879–11884.
21 T. Kiss, K. Gajda-Schrantz and P. F. Zatta, *Neurodegenerative Diseases and Metal Ions*, John Wiley & Sons, Ltd, 2006, ch. 13, pp. 371–393.
22 M. Abdel-ghany, A. Khalek and D. Shalloway, *J. Biol. Chem.*, 1993, **268**, 11976–11981.
23 C. Exley, *Coord. Chem. Rev.*, 2012, **256**, 2142–2146.
24 J. I. Mujika, J. Rodríguez-Guerra Pedregal, X. Lopez, J. M. Ugalde, L. Rodríguez-Santiago, M. Sodupe and J.-D. Maréchal, *Chem. Sci.*, 2017, **8**, 5041–5049.
25 L. Tomljenovic, *J. Alzheimers Dis.*, 2011, **23**, 567–598.
26 C. Exley, *Front. Neurol.*, 2014, **5**, 1–6.
27 V. B. Gupta, S. Anitha, M. L. Hegde, L. Zecca, R. M. Garruto, R. Ravid, S. K. Shankar, R. Stein, P. Shanmugavelu and K. S. Jagannatha Rao, *Cell. Mol. Life Sci.*, 2005, **62**, 143–158.
28 G. Crisponi, V. M. Nurchi, V. Bertolasi, M. Remelli and G. Faa, *Coord. Chem. Rev.*, 2012, **256**, 89–104.
29 T. Kiss, *J. Inorg. Biochem.*, 2013, **128**, 156–163.
30 R. A. Yokel, *Coord. Chem. Rev.*, 2002, **228**, 97–113.
31 G. Crisponi, A. Dean, V. Di Marco, J. I. Lachowicz, V. M. Nurchi, M. Remelli and A. Tapparo, *Anal. Bioanal. Chem.*, 2013, **405**, 585–601.
32 G. Crisponi, V. M. Nurchi, J. I. Lachowicz, M. Crespo-Alonso, M. A. Zoroddu and M. Peana, *Coord. Chem. Rev.*, 2015, **284**, 278–285.
33 A. E. Martell, R. D. Hancock, R. M. Smith and R. J. Motekaitis, *Coord. Chem. Rev.*, 1996, **149**, 311–328.
34 T. Kaur, R. K. Bijarnia and B. Nehru, *Drug Chem. Toxicol.*, 2009, **32**, 215–221.
35 T. Kiss, I. Sovago and R. B. Martin, *J. Am. Chem. Soc.*, 1989, **111**, 3611–3614.
36 T. Kiss, *Arch. Gerontol. Geriatr.*, 1995, **21**, 99–112.
37 A. C. Miu and O. Benga, *J. Alzheimers Dis.*, 2006, **10**, 179–201.
38 A. J. Cross, T. J. Crow, E. K. Perry, R. H. Perry, G. Blessed and B. E. Tomlinson, *Br. Med. J. (Clin. Res. Ed.)*, 1981, **282**, 93–94.
39 M. Milanese, M. I. Lkhayat and P. Zatta, *J. Trace Elem. Med. Biol.*, 2001, **15**, 139–141.
40 V. M. Nurchi, T. Pivetta, J. I. Lachowicz and G. Crisponi, *J. Inorg. Biochem.*, 2009, **103**, 227–236.

41 V. M. Nurchi, M. Crespo-Alonso, L. Toso, J. I. Lachowicz, G. Crisponi, G. Alberti, R. Biesuz, A. Dominguez-Martin, J. Niclos-Gutierrez, J. M. Gonzalez-Perez and M. A. Zoroddu, *J. Inorg. Biochem.*, 2013, **128**, 174–182.
42 A. Dean, E. Sija, E. Zsigo, M. G. Ferlin, D. Marton, V. Gandin, C. Marzano, D. Badocco, P. Pastore, A. Venzo, R. Bertani, T. Kiss and V. Di Marco, *Eur. J. Inorg. Chem.*, 2013, **2013**, 1310–1319.
43 A. Dean, M. G. Ferlin, P. Brun, I. Castagliuolo, R. A. Yokel, A. Venzo, G. Giorgio Bombi and V. B. Di Marco, *Inorg. Chim. Acta*, 2011, **373**, 179–186.
44 V. M. Nurchi, G. Crisponi, J. I. Lachowicz, S. Murgia, T. Pivetta, M. Remelli, A. Rescigno, J. Niclos-Gutierrez, J. M. Gonzalez-Perez, A. Dominguez-Martin, A. Castineiras and Z. Szewczuk, *J. Inorg. Biochem.*, 2010, **104**, 560–569.
45 O. Gutten and L. Rulisek, *Inorg. Chem.*, 2013, **52**, 10347–10355.
46 Q. Y. Wu, Y. T. Song, L. Ji, C. Z. Wang, Z. F. Chai and W. Q. Shi, *Phys. Chem. Chem. Phys.*, 2017, **19**, 26969–26979.
47 J. H. Lan, W. Q. Shi, L. Y. Yuan, J. Li, Y. L. Zhao and Z. F. Chai, *Coord. Chem. Rev.*, 2012, **256**, 1406–1417.
48 J. R. Pliego and J. M. Riveros, *J. Phys. Chem. A*, 2001, **105**, 7241–7247.
49 D. Riccardi, H. B. Guo, J. M. Parks, B. Gu, L. Liang and J. C. Smith, *J. Chem. Theory Comput.*, 2013, **9**, 555–569.
50 J. I. Mujika, E. Rezabal, J. M. Mercero, F. Ruipérez, D. Costa, J. M. Ugalde and X. Lopez, *Comput. Struct. Biotechnol. J.*, 2014, **9**, e201403002.
51 J. Tomasi, B. Mennucci and R. Cammi, *Chem. Rev.*, 2005, **105**, 2999–3093.
52 R. Lonsdale, J. N. Harvey and A. J. Mulholland, *J. Chem. Theory Comput.*, 2012, **8**, 4637–4645.
53 W. Hujo and S. Grimme, *J. Chem. Theory Comput.*, 2013, **9**, 308–315.
54 R. Sedlak, T. Janowski, M. Pitonak, J. Rezac, P. Pulay and P. Hobza, *J. Chem. Theory Comput.*, 2013, **9**, 3364–3374.
55 J. Alí-Torres, L. Rodríguez-Santiago and M. Sodupe, *Phys. Chem. Chem. Phys.*, 2011, **13**, 7852–7861.
56 R. F. W. Bader, *Atoms in Molecules: A Quantum Theory*, Oxford Univ. Press, Oxford, 1990.
57 K. Kitaura and K. Morokuma, *Int. J. Quantum Chem.*, 1976, **10**, 325–340.
58 T. Ziegler and A. Rauk, *Theor. Chim. Acta*, 1977, **46**, 1–10.
59 M. Giambiagi, M. S. de Giambiagi, C. D. dos Santos Silva and A. P. de Figueiredo, *Phys. Chem. Chem. Phys.*, 2000, **2**, 3381–3392.
60 P. Bultinck, R. Ponec and S. Van Damme, *J. Phys. Org. Chem.*, 2005, **18**, 706–718.
61 T. Kiss, K. Atkari, M. Jezowska-bojczuk and P. Decock, *J. Coord. Chem.*, 1993, **29**, 81–96.
62 R. Hider, *Thalassemia Rep.*, 2014, **4**, 19–27.
63 G. Crisponi and M. Remelli, *Coord. Chem. Rev.*, 2008, **252**, 1225–1240.
64 C. Bazzicalupi, A. Bianchi, C. Giorgi, M. P. Clares and E. Garcia-Espana, *Coord. Chem. Rev.*, 2012, **256**, 13–27.
65 G. Gervasio, R. Bianchi and D. Marabello, *Chem. Phys. Lett.*, 2004, **387**, 481–484.
66 T. S. Koritsanszky and P. Coppens, *Chem. Rev.*, 2001, **101**, 1583–1628.
67 B. Silvi and C. Gatti, *J. Phys. Chem. A*, 2000, **104**, 947–953.
68 E. Matito, M. Solà, P. Salvador and M. Duran, *Faraday Discuss.*, 2007, **135**, 325–345.
69 F. Feixas, E. Matito, J. Poater and M. Solà, *Chem. Soc. Rev.*, 2015, **44**, 6434–6451.
70 R. G. Pearson, *J. Am. Chem. Soc.*, 1963, **85**, 3533–3539.
71 R. Milacic, S. Murko and J. Scancar, *J. Inorg. Biochem.*, 2009, **103**, 1504–1513.
72 P. Rubini, A. Lakatos, D. Champmartin and T. Kiss, *Coord. Chem. Rev.*, 2002, **228**, 137–152.